

# A QED Model for Non-thermal Emission from SGRs and AXPs

Jeremy S. Heyl<sup>1</sup>

*Department of Physics and Astronomy, University of British Columbia 6224 Agricultural Road, Vancouver,  
British Columbia, Canada, V6T 1Z1*

Lars Hernquist

*Harvard-Smithsonian Center for Astrophysics, MS-51, 60 Garden Street, Cambridge, Massachusetts 02138,  
United States*

## ABSTRACT

Previously, we showed that, owing to effects arising from quantum electrodynamics (QED), magnetohydrodynamic fast modes of sufficient strength will break down to form electron-positron pairs while traversing the magnetospheres of strongly magnetised neutron stars. The bulk of the energy of the fast mode fuels the development of an electron-positron fireball. However, a small, but potentially observable, fraction of the energy ( $\sim 10^{33}$  ergs) can generate a non-thermal distribution of electrons and positrons far from the star. In this paper, we examine the cooling and radiative output of these particles. We also investigate the properties of non-thermal emission in the absence of a fireball to understand the breakdown of fast modes that do not yield an optically thick pair plasma. This quiescent, non-thermal radiation associated with fast mode breakdown may account for the recently observed non-thermal emission from several anomalous X-ray pulsars and soft-gamma repeaters.

## 1. Introduction

Soft gamma repeaters (SGRs) and anomalous X-ray pulsars (AXPs) comprise a subclass of neutron stars with unusual properties compared to typical radio pulsars. The dozen or so known SGRs and AXPs emit pulsed X-rays, with steadily increasing periods, as well as bursts of hard X-rays and soft  $\gamma$ -rays at irregular intervals, spin slowly, and appear to be radio quiet. Compared with high-mass X-ray binaries, SGRs and AXPs have relatively low X-ray luminosities, soft spectra, and no detectable companions (for reviews, see, e.g. Hurley 2000; Mereghetti et al. 2002).

While it seems clear that SGRs and AXPs cannot be rotation-powered, their ultimate energy source remains unclear. In the “magnetar” model (Duncan & Thompson 1992; Thompson & Duncan 1995), these objects are ultramagnetised neutron stars with fields  $B_* \sim 10^{14} - 10^{15}$  G, fueled by either magnetic field decay (Thompson & Duncan 1996; Heyl & Kulkarni 1998) or residual thermal energy (Heyl & Hernquist 1997c,d). Alternatively, these stars may have “ordinary” field strengths  $B_* \sim 10^{11} - 10^{13}$  G and be powered by accretion from e.g. a fossil disk (Corbet et al. 1995; Chatterjee et al. 2000; Alpar 2001; Menou et al. 2001), but recent analyses indicate that disks of the required mass may not survive sufficiently long around these stars (e.g. Ekşi et al. 2005).

According to the magnetar model, bursts occur when fractures in the crust of the star send Alfvén waves into the magnetosphere (Thompson & Duncan 1995). In earlier work, we analysed wave propagation

---

<sup>1</sup>Canada Research Chair

through fields exceeding the quantum critical value  $B_{\text{QED}} \equiv m^2 c^3 / e \hbar \approx 4.4 \times 10^{13}$  G, and demonstrated circumstances under which electromagnetic (Heyl & Hernquist 1998) and some MHD waves, particularly fast modes (Heyl & Hernquist 1999) evolve in a non-linear manner and eventually exhibit discontinuities similar to hydrodynamic shocks, owing to vacuum polarisation from quantum electrodynamics (QED). In Heyl & Hernquist (2005, hereafter Paper I), we developed a theory to account for bursts from SGRs and AXPs based on “fast-mode breakdown,” in which wave energy is dissipated into electron-positron pairs when the scale of these discontinuities becomes comparable to an electron Compton wavelength. We showed that, under appropriate conditions, an extended, optically thick pair-plasma fireball would result, radiating primarily in hard X-rays and soft  $\gamma$ -rays.

Our mechanism provides a natural and efficient outlet for ultramagnetised neutron stars to form bursts of high energy radiation without significant emission at shorter wavelengths. However, as we noted in Paper I, non-thermal electrons and positrons would be produced far from the star, beyond the optically thick fireball, radiating over a wide range of frequencies. In addition, MHD fast modes of insufficient amplitude to generate an optically thick fireball will still dissipate through pair-production, seeding non-thermal emission.

In what follows, we extend our previous investigation of fast-mode breakdown to estimate the spectrum of non-thermal emission expected outside the region containing an optically thick fireball. We also consider the fate of fast modes which dissipate their energy through pair production but at a rate insufficient to yield a fireball. We show that when a fireball is generated with sufficient energy to account for the thermal radiation associated with bursts from SGRs or AXPs, small, but detectable amounts of non-thermal emission are predicted which dominate the spectrum both well below and well above X-ray energies. Our model makes a specific prediction for the spectral energy distribution of the non-thermal component that can be used to test our theory for SGR and AXP bursts.

For weaker fast modes that do not yield an optically thick fireball, we show that the non-thermal radiation may be sufficient to explain the quiescent, non-thermal emission observed recently from several SGRs and AXPs. Therefore, our model naturally provides a unified explanation for several of the unique characteristics of SGRs and AXPs in the context of the magnetar scenario.

## 2. Calculations

In Paper I, we assumed that the energy dissipated from the fast mode fuels a pair fireball. This assumption is reasonable as long as the region is opaque to X-rays. Any electrons and positrons produced will generate synchrotron radiation which will be scattered and form additional pairs in the strong magnetic field. Beyond about one hundred stellar radii, the synchrotron radiation can escape without becoming thermalised. Although it may suffer synchrotron self-absorption, a power-law distribution of electrons and positrons can radiate outside the fireball, and we would expect a synchrotron radiation spectrum.

### 2.1. Primary Pairs and Photons

Below, we examine our model from Paper I in the limit when the pair plasma does not thermalise. As fast modes produced near the stellar surface propagate outwards, they develop strong discontinuities (shocks) when the magnetic field is sufficiently large and the wave energy will eventually be dissipated through pair production. If we consider the situation when the electron-positron distribution is no longer

thermal, we must adopt some model for the energies of these particles when they are created. A simple and reasonable assumption is that they are nearly at rest in the frame of the shock as they are produced. In the ultrarelativistic limit, this is required in order to conserve both momentum and energy as the wave dissipates.

The shock is ultrarelativistic and travels at the speed of light in the strong magnetic field. The non-thermal pairs are produced far from the star where it is appropriate to use the weak-field limit of the index of refraction,

$$n_{\perp} \approx 1 + \frac{\alpha_f}{4\pi} \frac{8}{45} \left( \frac{B}{B_{\text{QED}}} \right)^2, \quad (1)$$

where  $\alpha_f \equiv e^2/\hbar c$  is the fine-structure constant, and so

$$\gamma = \frac{1}{\sqrt{1-\beta^2}} \approx \frac{1}{\sqrt{2(1-\beta)}} \approx \frac{3}{2} \sqrt{\frac{5\pi}{\alpha_f}} \frac{B_{\text{QED}}}{B} \quad (2)$$

where  $B_{\text{QED}} \equiv m^2 c^3 / (e \hbar) \approx 4.4 \times 10^{13}$  G. (We note that the derivation of the effective Lagrangian of QED presented by Heyl & Hernquist (1997a), valid for any magnetic field strength, correctly reduces to the weak field limit of e.g. Heisenberg & Euler (1936), yielding the above expression for the index of refraction (Heyl & Hernquist 1997b).)

Paper I describes in detail how the energy is dissipated as the fast mode travels away from the stellar surface. Here, we are interested in the evolution of the wave in the weak-field limit, far from the star, so we can obtain simple relationships for the amount of energy released as a function of the distance from the surface. The emission from outside a particular radius is proportional to  $(kb)^{-2} r^{-3}$  where  $k$  is the initial wavenumber of a fast-mode wave,  $b$  is its initial amplitude compared to the magnetic field of the star, and  $r$  is the distance from the star, so we have

$$dE = A r^{-4} dr, \quad (3)$$

where the constant  $A$  must be determined from modeling the evolution of the wave near the neutron star, as described in Paper I.

At each radius from the star, we assume that the pair spectrum is monoenergetic, so the total emission is the sum of contributions from different electron-positron energies traveling in different strengths of magnetic field. The particles more distant from the star have higher typically energies and also travel through weaker fields.

We explicitly add the radial dependence to the Lorentz factor of the particles and calculate the Larmor radius of the particles as a function of distance from the star.

$$\gamma \approx 70 \frac{B_{\text{QED}}}{B_*} \left( \frac{r}{R} \right)^3, \quad (4)$$

where  $R$  is the radius of the star, and  $B_*$  is the pole field strength at the stellar surface, so

$$r_{\text{Larmor}} \approx \frac{\gamma m c^2}{e B} = \frac{3}{2} \sqrt{\frac{5\pi}{\alpha_f}} \left( \frac{B}{B_{\text{QED}}} \right)^{-2} \frac{\hbar}{m c} = 2.6 \times 10^{-15} r R_6^{-1} \left( \frac{r}{R} \right)^5 \left( \frac{B_*}{B_{\text{QED}}} \right)^{-2}, \quad (5)$$

where  $R_6$  is the radius of the star in units of  $10^6$  cm, and we see that particles produced closer than a thousand stellar radii are essentially trapped. From Paper I, we find that the fireball extends to about one

hundred stellar radii, so our region of interest spans an order of magnitude in distance but three orders of magnitude in magnetic field strength and particle energy.

If classical synchrotron radiation is important, the emission at each radius will extend approximately up to photon energies of

$$\hbar\omega = \gamma^2 \hbar\omega_B = \gamma^2 \frac{eB}{mc} \approx \frac{45}{4} \frac{\pi}{\alpha_f} \frac{B_{\text{QED}}}{B} mc^2, \quad (6)$$

where  $\hbar\omega_B$  is the non-relativistic cyclotron energy.

We can estimate the recoil on the electron owing to the emission of individual photons

$$\chi = \frac{\hbar\omega}{\gamma mc^2} = \gamma \frac{B}{B_{\text{QED}}} = \frac{3}{2} \sqrt{\frac{5\pi}{\alpha_f}} \approx 70 \gg 1, \quad (7)$$

and, so, we must treat the synchrotron emission quantum mechanically.

According to the results of Berestetskii et al. (1982), the emission peaks at a energy

$$E_{\text{peak}} = \frac{1}{2} \hbar\omega_c = \frac{1}{2} \gamma mc^2 \frac{\chi}{\frac{2}{3} + \chi} \approx \frac{1}{2} \gamma mc^2 = \frac{3}{4} \sqrt{\frac{5\pi}{\alpha_f}} \frac{B_{\text{QED}}}{B} mc^2. \quad (8)$$

The power radiated by the electron is given by

$$I \approx \frac{32\Gamma(\frac{2}{3})}{243} \alpha_f (3\chi)^{2/3} \frac{(mc^2)^2}{\hbar} \approx 0.05 \frac{(mc^2)^2}{\hbar} \quad (9)$$

so the electrons and positrons lose their initial energy over  $\sim 20\gamma$  Compton wavelengths and the primary radiation is strongly beamed parallel to the direction of the fast wave.

## 2.2. Formation of Secondary Particles

The high-energy synchrotron photons passing through the strong magnetic field may produce pairs through one-photon pair-production. It is reasonable to assume that  $\hbar\omega \gg mc^2$  (Eq. 8), so we will use the results of Berestetskii et al. (1982). The key parameter is essentially

$$\kappa = \frac{\hbar^2 e B \omega}{m^3 c^5} = \frac{B}{B_{\text{QED}}} \frac{\hbar\omega}{mc^2} \approx \frac{\chi}{2} = \frac{3}{4} \sqrt{\frac{5\pi}{\alpha_f}} \approx 35 \gg 1, \quad (10)$$

where we have used the value of  $\omega_c$  from Eq. (6). Therefore, we can use the large  $\kappa$  limit of the pair-production rate

$$w = \frac{5\Gamma^2(\frac{2}{3})}{7\pi^{1/2}\Gamma(\frac{7}{6})} \frac{3^{1/6}}{2^{4/3}} \alpha_f \frac{B}{B_{\text{QED}}} \frac{mc^2}{\hbar} \kappa^{-1/3} \approx 8.5 \times 10^{-4} \frac{mc^2}{\hbar} \frac{B}{B_{\text{QED}}}. \quad (11)$$

These secondary pairs will typically have energies one-quarter that of the first generation of particles. The fourth generation of particles will have energies typically  $4^{-3}$  or 64 times smaller than the first generation. This fourth generation will have  $\chi \sim 1$  so the typical energy of the resulting synchrotron photons will be less than one-half the energy of the pairs so  $\kappa \ll 1$ , quenching the pair production rate,

$$w = \frac{3^{3/2}}{2^{9/2}} \alpha_f \frac{B}{B_{\text{QED}}} \frac{mc^2}{\hbar} e^{-8/3\kappa}. \quad (12)$$

We assume that that  $c/w \lesssim r$  for pair production to be effective. We find that the pair-production quenches for

$$\kappa \sim 0.1 \left[ 1 + 0.04 \ln \left( \frac{r}{10^8 \text{ cm}} \frac{B}{10^{-5} B_{\text{QED}}} \right) \right]^{-1}. \quad (13)$$

To calculate the final spectrum of radiation, we will make the ansatz that only the final generation of pairs contributes to the observed emission and that their energies are about half the energy of the last generation of pair-producing photons, so they have  $\chi \approx \kappa/2 \sim 0.04$ . Using the definition of  $\chi$  we find

$$\gamma = \chi \frac{B_{\text{QED}}}{B} = 0.05 \frac{B_{\text{QED}}}{B}. \quad (14)$$

If we compare this result with Eq. (2), we find that the energy of the pairs has been degraded by a factor of about 1700.

Because  $\chi \ll 1$  we can assume that the emission is classical. The emission will have typical energies of

$$\hbar\omega_t = \gamma^2 \hbar\omega_B \approx 2.5 \times 10^{-3} \frac{B_{\text{QED}}}{B} mc^2. \quad (15)$$

We can combine Eq. (3) with Eq. (15) to obtain an estimate of the spectrum of resulting photons,

$$dE \propto r^{-6} dE_\gamma \propto E_\gamma^{-2} dE_\gamma \text{ for } E_\gamma > E_{\text{break}}, \quad (16)$$

where  $E_{\text{break}}$  is the value of Eq. (15) at the edge of the fireball.

A final important element is the cooling time of the final generation of pairs:

$$\tau_{\text{cool}} = \frac{\gamma mc^2}{\frac{2}{3} r_0^2 c \beta_\perp^2 \gamma^2 B^2} \approx \frac{30}{\alpha_f} \frac{B_{\text{QED}}}{B} \frac{\hbar}{mc^2}, \quad (17)$$

where  $r_0 \equiv e^2/mc^2$  is the classical electron radius, and so the final generation of pairs cools nearly immediately. The pairs closest to the surface of the star have the lowest energy and cool the most quickly, so for lower energies we have

$$dE \propto E_\gamma^{-1/2} dE_\gamma \text{ for } E_0 < E_\gamma < E_{\text{break}}, \quad (18)$$

where  $E_0 = \hbar\omega_{B,\text{FB}}$  is the non-relativistic cyclotron energy at the outer edge of the fireball. Below this energy we observe radiation from the pairs formed further away from the surface of the star. There are fewer of these pairs, but because they form in a weaker magnetic field their spectra will extend to lower energies.

The spectra of these electrons extends as  $E^{-1/2}$  from  $E_{\text{break}} B_{\text{FB}}/B$  down to  $E_0 B/B_{\text{FB}}$  but the normalisation is smaller by  $(B/B_{\text{FB}})^2$  so we have

$$dE \propto E_\gamma dE_\gamma \text{ for } E_{\text{min}} < E_\gamma < E_0, \quad (19)$$

where  $E_{\text{min}}$  is the cyclotron energy at the radius where the pairs are no longer trapped from Eq. 5.

Putting together Eq. (16), (18) and (19) and normalising by the total energy in non-thermal radiation yields the complete spectrum

$$\frac{dE}{dE_\gamma} = \frac{E_{\text{total}}}{3E_{\text{break}}} \begin{cases} \frac{E_\gamma}{E_{\text{break}}} \left( \frac{E_{\text{break}}}{E_0} \right)^{3/2}, & E_{\text{min}} < E_\gamma < E_0 \\ \left( \frac{E_\gamma}{E_{\text{break}}} \right)^{-1/2}, & E_0 < E_\gamma < E_{\text{break}} \\ \left( \frac{E_\gamma}{E_{\text{break}}} \right)^{-2}, & E_{\text{break}} < E_\gamma < E_{\text{max}} \end{cases} \quad (20)$$

where  $E_{\min}$  and  $E_{\max}$  are determined by the non-relativistic cyclotron frequency and the typical emission energy, given in Eq. 16 at the outer edge of the region where the primary pairs are initially trapped by the field from Eq. 5. Typically,  $E_{\min} \sim 10^{-3}E_0$  and  $E_{\max} \sim 10^3 E_{\text{break}}$ . To find the normalisation in Eq. (20), we have assumed that  $E_{\max} \gg E_{\text{break}}$  and  $E_0 \ll E_{\text{break}}$

The bulk of the energy emerges near  $E_{\text{break}}$ , and the bulk of the photons have energies near  $E_0$ , and the mean energy of a photon is

$$\sqrt{E_{\text{break}}E_0} = \chi mc^2 = 0.05 mc^2, \quad (21)$$

where  $\chi$  is given in Eq. (14).

We now estimate the values of  $E_0$  and  $E_{\text{break}}$ . From the models presented in Paper I, we have  $r_{\text{FB}} \approx 100R$ , so

$$E_0 \approx 10^{-6} \frac{B_*}{B_{\text{QED}}} mc^2 \approx 5 \text{ eV} \text{ and } E_{\text{break}} \approx 1600 \frac{B_{\text{QED}}}{B_*} mc^2 \approx 80 \text{ MeV}, \quad (22)$$

where the final results assume that  $B_* = 10B_{\text{QED}}$ . The mean photon energy is around 25 keV. In Paper I, we argued that about  $10^{34}$  ergs per burst may go into non-thermal emission. In this case, we would have approximately  $2.5 \times 10^{41}$  photons or  $2 \times 10^{-3}$  photons per square centimeter at a distance of 10 kpc. The bulk of the photons will have energies around  $E_0$ .

The total energy in the non-thermal emission is proportional to the value of the magnetic field at the edge of the fireball (from Eq. 3), so as one can see from Fig. 1, the high-energy spectrum simply extends to a lower value of  $E_{\text{break}}$  and the low-energy spectrum extends to a higher value of  $E_0$  as the radius of the fireball decreases.

### 2.3. Time Dependence of Spectral Emission

Fig. 1 gives the total spectrum of radiation, both thermal and non-thermal from the burst, integrated over time. While the pairs are still relativistic we find that the cooling time is

$$\tau_{\text{cool}} = \frac{3}{2} \left( \frac{E_t}{mc^2} \frac{B}{B_{\text{QED}}} \right)^{-1/2} \frac{\hbar}{mc^2} \quad (23)$$

as a function of the energy of the typical synchrotron photon  $E_t$ . If we compare this result with Eq. (15), we find that initially the typical photon energy is also inversely proportional to the field strength, so as time passes we have a spectrum  $F_E \propto E_\gamma^{-2}$  above a frequency  $E_{\text{break}}(t) \propto t^{-2}$ . The value of  $F_E$  at  $E_{\text{break}}(t)$  is independent of time.

The pairs produced nearest to the star become non-relativistic first so as  $E_{\text{break}}$  approaches  $E_0$  the spectrum steepens and at late times approaches  $F_E \propto E_\gamma$ , but now the normalisation decreases rapidly with time. To appreciate the rate of cooling we can substitute a value for  $E_0$  into the cooling time Eq. (23) to get

$$\tau_{\text{cool}} = \frac{3}{2} \frac{B_{\text{QED}}}{B} \frac{\hbar}{mc^2} \quad (24)$$

so the pairs cool very rapidly to non-relativistic energies over  $10^{5-8}$  Compton times or 0.1 to 10 femtoseconds. Observationally, one expects to see the non-thermal spectrum as depicted in Fig. 1 immediately before the fireball radiation ( $\sim 10^{-3}$  s). The non-thermal emission dominates the fireball emission both at low energies and for  $E_\gamma \gg kT_{\text{FB}}$

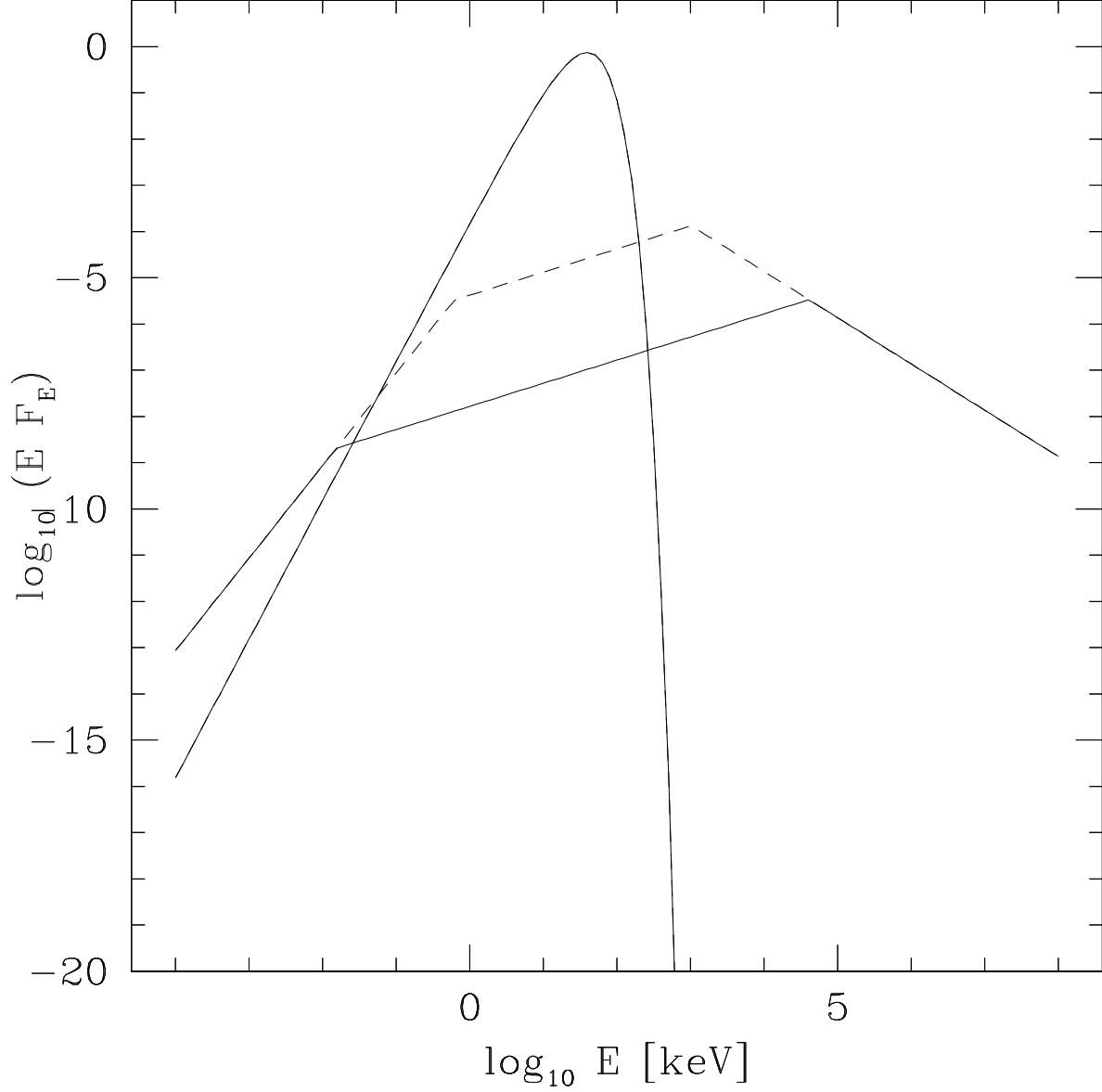


Fig. 1.— Spectrum from an SGR or AXP fireball (smooth solid curve) compared with the non-thermal emission.  $T_{FB} = 10$  keV and the non-thermal emission comprises  $10^{-5}$  of the fireball energy. The value of the magnetic field at the edge of the fireball (100 stellar radii) is taken to be  $3 \times 10^{-5} B_{\text{QED}}$ , yielding  $E_0 = 15$  eV and  $E_{\text{break}} = 40$  MeV (broken solid line). If the fireball ends at thirty stellar radii,  $E_0$  and  $E_{\text{break}}$  increase and decrease respectively by a factor of 25000 and the total non-thermal energy is  $3 \times 10^{-4}$  of the fireball emission (dashed line). As we argue in § 2.7, values of  $E_{\text{break}}$  less than 1 MeV do not make sense physically, so the fast-mode cascade as we have described is limited to fields less than  $\approx 10^{-3} B_{\text{QED}}$ , well within the weak-field limit.

## 2.4. Inverse-Compton versus Synchrotron Power

We have assumed implicitly that synchrotron emission dominates the energy loss of the high energy pairs produced in the cascade. If we assume that the fireball emits  $10^{40}$  erg/s we can estimate the photon energy density:

$$U_{\text{photon}} = \frac{L}{4\pi r^2 c} = 2 \times 10^{12} L_{40} r_8^{-2} \text{ erg cm}^{-3} \quad (25)$$

and the magnetic energy density

$$U_B = \frac{B^2}{8\pi} = 4 \times 10^{16} B_{*,15}^2 r_8^{-6} \text{ erg cm}^{-3} \quad (26)$$

so

$$\frac{P_{\text{IC}}}{P_{\text{Sych}}} = \frac{U_{\text{photon}}}{U_B} = 5 \times 10^{-6} L_{40} r_8^4 B_{*,15}^{-2}. \quad (27)$$

Inverse-Compton emission may be important for  $r \gg 10^9$  cm. Coincidentally, this is the same distance from the star where the Larmor radius of the initial pairs becomes greater than the distance from the star (Eq. 5), where synchrotron emission is not very effective. Regardless, the total energy deposited in this outermost region is  $10^{-3}$  lower than the synchrotron-dominated region (Eq. 3).

In principle, the larger bursts such as the March 7 and August 28 events have sufficient luminosity to make inverse Compton emission important. However, the cooling time for the pairs (Eq. 17) is so short that the pairs will lose most of their initial energy before the fireball radiation reaches the non-thermal emitting region. The cooling time for pairs emitting at lower energies is sufficiently long that inverse-Compton emission might be important for these electrons in the brightest SGR bursts.

## 2.5. Two-photon Pair Production

To determine the efficacy of two-photon pair production we must first decide whether the highest energy photons produced in the cascade (Eq. 8) lie above the threshold to interact with the thermal photons from the neutron star or other ambient photons. The photons produce by the fireball simply do not catch up with the photons produced in the cascade.

For the thermal photons, we must have

$$E_{\text{CM}} = \sqrt{E_{\text{peak}} E_{\text{thermal}} (1 - \cos \theta)} \approx 0.133 \left( \frac{E_{\text{thermal}}}{1 \text{ keV}} \frac{B_{\text{QED}}}{B_*} \frac{r}{R} \right)^{1/2} \text{ MeV} > 1 \text{ MeV} \quad (28)$$

so for

$$r > 60 \frac{B_*}{B_{\text{QED}}} \left( \frac{E_{\text{thermal}}}{1 \text{ keV}} \right)^{-1} R \quad (29)$$

two-photon pair production may operate. However, the cascade typically dumps most of its energy around  $r = 100R$  and  $B_* \gtrsim 10B_{\text{QED}}$  so two-photon pair production against the thermal photons from the neutron star lies below threshold. Furthermore, even if the thermal photons were above threshold, the mean-free path is greater than  $10^3 R$  and much much greater than the mean-free path for one-photon pair production.

We can repeat the calculation for ambient photons from starlight

$$E_{\text{CM}} = \sqrt{E_{\text{peak}} E_{\text{ambient}}} = 4 \times 10^{-3} \left( \frac{E_{\text{ambient}}}{1 \text{ eV}} \frac{B_{\text{QED}}}{B_*} \frac{r^3}{R^3} \right)^{1/2} \text{ MeV} \quad (30)$$



so

$$r > 40 \left( \frac{B_*}{B_{\text{QED}}} \right)^{1/3} \left( \frac{E_{\text{ambient}}}{1 \text{ eV}} \right)^{-1/3} R. \quad (31)$$

The ambient starlight typically does have sufficient energy to pair-produce against the first generation of photons produced in the cascade but the mean-free path is from kiloparsecs to megaparsecs much greater than the scale of the cascade region.

## 2.6. The Fast-Mode Cascade Contrasted with the Pulsar Cascade

The main difference between the fast-mode cascade and the pair-cascade invoked to explain pulsar emission is geometry. The pulsar cascade is instigated by charged particles that are restricted to travel along magnetic field lines – any perpendicular momentum is quickly reduced through synchrotron emission. The photons that are produced also travel nearly parallel to the field lines, so photons must travel some fraction of the curvature length of the magnetic field before their momentum perpendicular to the magnetic field is sufficient to produce a pair. Consequently, the pairs are produced nearly on threshold.

The fast-mode is not restricted to travel along the field lines. Here, we have explicitly assumed that it travels perpendicular to the field lines. Regardless of the precise angle, the pairs produced initially will have much of their momentum perpendicular to the field resulting in many photons traveling perpendicular to the field that can in principle produce pairs *in situ*. What quenches the process is the reduction of the cross-section as the energy of the subsequent photon generations decreases.

## 2.7. The Fast-Mode Cascade without SGR Bursts

In Paper I, we argued that a sufficiently widespread production of fast modes would result in the creation of a fireball because the vicinity of the star would be opaque to X-rays simply owing to the Thomson cross section of the pairs. The optical depth between the surface of the star and infinity is simply proportional to the fraction of the star’s surface area generating magnetohydrodynamic waves. The SGR bursts typically involve a large surface area  $\sim R^2$  emitting fast-modes with a fractional amplitude of several percent within several light-crossing times of the inner magnetosphere.

These large-scale events are bound to be rare. On the other hand, smaller scale stresses in the crust of the star may be relieved more regularly. This would excite only a small fraction of the neutron star surface, but in principle the amplitude of the waves might be sufficient to cause fast-mode breakdown. In this case, all of the radiation produced would follow the non-thermal distribution outlined in this paper.

What would be the typical flux of these small-scale fast modes? Thompson & Duncan (1996) and Heyl & Kulkarni (1998) have argued that the quiescent emission of SGR and AXP neutron stars may be powered by the decay of the magnetic field. The quiescent thermal emission may only be a small fraction of the total energy released by the decay of the magnetic field. Recent observations of SGRs and AXPs indicate that the thermal radiation may indeed be just the tip of the iceberg (Molkov et al. 2004; Mereghetti et al. 2004a; Kuiper et al. 2004); therefore, we will be liberal in our assumption of the relative amplitude of the thermal and non-thermal radiation and allow the pair cascade to operate beyond a certain radius from the star or equivalently below a certain magnetic field strength ( $B_{\text{max}}$ ). This model has two parameters,  $B_{\text{max}}$  determines the position of the two breaks in the spectrum and the total normalisation. The process

of fast-mode breakdown predicts a particular relationship between the location of the two breaks in the spectrum (22) and particular slopes (20) between and beyond the breaks.

Figure 2 shows the observed broad-band spectrum of several AXPs and SGRs. To compare the spectra we have placed the more distant objects (AXP 1E 1841-045 and SGR 1806-20) whose hard X-ray emission was discovered with INTEGRAL at the distance of 4U 0142+61 whose optical emission (Hulleman et al. 2000) is very likely to be nonthermal (Özel 2004).

Because the location of the two breaks in the spectrum both depend on the strength of the magnetic field at the inner edge of the breakdown region, we find that the presence of extensive nonthermal optical emission indicates that the non-thermal hard X-ray emission should peak at about 30 MeV, a factor of two hundred beyond the observed spectrum. The best limits in this energy range are provided by EGRET.

We come to this conclusion under the assumption that SGR 1806-20 and AXP 1E 1841-045 have a similar optical excess to 4U 0141+61. A more conservative assumption would be that the hard X-ray emission does not extend far beyond the observations from INTEGRAL with spectral breaks at about 1 MeV and 650 eV. This situation is somewhat natural. The fast-mode cascade is limited to pairs with sufficient energy to produce photons with  $E > 1$  MeV that can subsequently pair produce. Lower energy electrons simply cool, giving the observed cooling spectrum in the hard X-rays. The total energy in the non-thermal emission is also reduced by a factor of a few. In the context of the fast-mode cascade it is difficult to have  $E_{\text{break}} < 2mc^2$ . This model is denoted as the “Minimal Model” in Fig. 2 because  $E_{\text{break}}$  takes on the minimal value that makes sense physically; i.e  $\approx 1$  MeV.

We can also obtain a conservative picture for AXP 4U 0142+61 by accounting for only the optical excess and getting a prediction for the hard X-ray emission. We assume that  $E_0$  is a few electron volts giving  $E_{\text{break}}$  on the order of 200 MeV. The minimal hard X-ray emission required to account for the optical emission is depicted in Figure 2 as the “Optical Model”. This optical model agrees well with the results reported by den Hartog et al. (2004). On the other hand, if AXP 4U 0142+61 has inherent non-thermal emission as strong as either AXP 1E 1841-045 or SGR 1806-20, the EGRET flux would be larger as given under the “Unified Model” in Table 1.

Table 1 gives the predicted EGRET fluxes above 100 MeV for the various objects and models. The optical model and the unified model predict approximately similar EGRET fluxes for 4U 0142+61. The minimal model based solely on the INTEGRAL data exhibits a flux above 100 MeV about two hundred times smaller than the unified model. Because the optical model cannot explain the observed INTEGRAL data for 1E 1841-045 and SGR 1806-20, it is omitted. Similarly, the minimal model cannot explain the optical data for 4U 0142+61. We see that for 1E 1841-045 and SGR 1806-20 the predictions for the minimal

Table 1: Predicted flux above 100 MeV and observed EGRET upper limits (Grenier & Perrot 2005) in units of  $10^{-8}$  photons  $\text{s}^{-1}\text{cm}^{-2}$ . The GLAST upper limits are nominally  $(0.2 - 0.4) \times 10^{-8}$  photons  $\text{s}^{-1}\text{cm}^{-2}$  (GLAST Facilities Science Team 1999).

Object	EGRET Exposure [weeks]	EGRET Upper Limit	Unified Model	Minimal Model	Optical Model
AXP 4U 0142+61	8.8	50	1500	—	800
AXP 1E 1841-045	6.8	70	70	0.4	—
SGR 1806-20	4.9	70	280	0.6	—

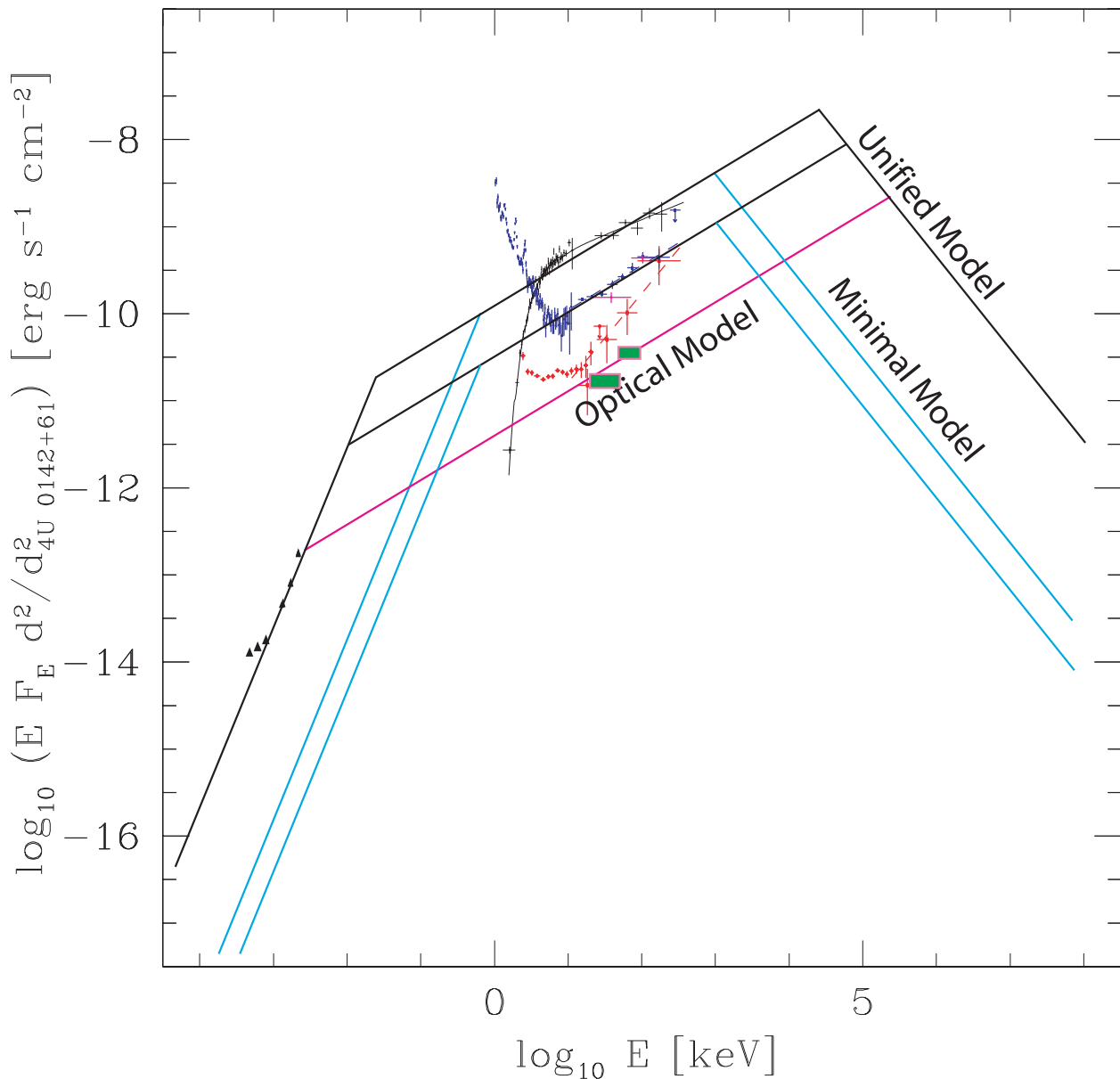


Fig. 2.— The spectrum produced by fast-mode breakdown is superimposed over the observed thermal and non-thermal emission from several AXPs and SGRs for models that fit either the optical or INTEGRAL data solely and one that fits both sets of data. The unabsorbed optical data are from Hulleman et al. (2000) via Özel (2004) for AXP 4U 0142+61. The uppermost black symbols are the hard X-ray band are from Molkov et al. (2004) for SGR 1806-20. Mereghetti et al. (2004a) obtained similar results for the SGR. The middle sets of points in the hard X-ray data (blue is total flux and red is pulsed flux) are from Kuiper et al. (2004) for AXP 1E 1841-045. The green squares plot the INTEGRAL data reported by den Hartog et al. (2004) for AXP 4U 0142+61. We normalised the den Hartog et al. (2004) results using the observations of the Crab by Jung (1989). We scaled the emission from the three sources by assuming that they all lie at the distance of AXP 4U 0142+61. We used 3 kpc for AXP 4U 0142+61 (Hulleman et al. 2000), 7.5 kpc for AXP 1E 1841-045 (Sanbonmatsu & Helfand 1992) and 15 kpc for SGR 1806-20 (Molkov et al. 2004).

model lie comfortably below the EGRET upper limits. In the context of the fast-mode breakdown model, this means that the optical emission for 1E 1841-045 and SGR 1806-20 is inherently weaker than from 4U 0142+61.

On the other hand, 4U 0142+61 is difficult to explain in the context of either model because of its large optical flux. Perhaps 4U 0142+61 was more active during the epoch of the optical observations than during the EGRET observations. Some AXPs exhibit variable X-ray emission such as AX J1845-0258 and 1E 1048.1-5937 (Vasisht et al. 2000; Mereghetti et al. 2004b) so this conclusion might be natural.

### 3. Discussion

We have presented a model for the non-thermal emission from AXPs and SGRs. It is a natural extension of the model for bursts that we presented in Paper I. When a dislocation of the surface of the neutron star is sufficiently large, the resulting fast modes will produce sufficient pairs to make the inner magnetosphere of the neutron star opaque to x-rays, generating a fireball. Some small but observable fraction of the energy initially in the fast modes is dissipated outside the opaque region yielding a characteristic fast-mode breakdown spectrum. A second possibility is that the crust of the neutron star is constantly shifted over small scales, generating fast modes whose breakdown is insufficient to produce a fireball. In this case we would associate the non-thermal radiation with the quiescent thermal radiation from the surface of the star.

The exponential quenching of one-photon pair production and the dipole geometry of the neutron star field at large distances constrains the spectrum produced by fast-mode breakdown to have only two free parameters. The cyclotron energy ( $E_0$ ) at the inner edge of the breakdown region (or alternatively  $E_{\text{break}}$ ) and the normalisation of the spectrum. The model does not yield any freedom in setting the spectral slope. Below  $E_0$ ,  $EF_E$  is proportional to  $E$ . Between  $E_0$  and  $E_{\text{break}}$  it is proportional to  $E^{1/2}$  and above  $E_{\text{break}}$   $EF_E \propto E^{-1}$ .

Because of the paucity of free parameters, our model has great predictive power, if one can ascribe the observed flux from an AXP or SGR to fast-mode breakdown. In the case of 4U 0141+61 whose optical and near infrared flux has been determined (Hulleman et al. 2000), the hard X-ray flux from fast-mode breakdown should be at least as large as found by den Hartog et al. (2004). Additionally, we have several predictions for the gamma-ray flux from AXPs and SGRs. Regardless of which model one assumes, the emission should extend beyond observed INTEGRAL data without a break below 1 MeV. Further INTEGRAL observations of these objects may verify this claim. If the object has a significant optical excess, such as 4U 0141+61, we predict that  $EF_E$  should continue to rise to 10 – 200 MeV, well into the realm of GLAST. Even the least favourable “Minimal” model for AXP 1E 1841-045 and SGR 1806-20 yields a marginal detection with GLAST.

Observations of the AXPs and SGRs continue to surprise, as do theoretical investigations of ultramagnetised neutron stars. In this paper and Paper I we have presented a unified model for the thermal burst emission and non-thermal emission from ultramagnetised neutron stars. The model has few underlying assumptions: magnetars produce fast modes sufficient to power the non-thermal emission and, more rarely, the bursts, the magnetic field far from the star is approximately dipolar and quantum electrodynamics can account for the dynamics of pairs and photons in strong magnetic fields. The model for the non-thermal emission has two free parameters, a normalisation and break frequency. Further observations can easily verify or falsify this model and potentially provide direct evidence for the ultramagnetised neutron stars that power AXPs and SGRs and the macroscopic manifestations of QED processes that account for their unique

attributes.

J.S.H. would like to thank Alice Harding for help with the EGRET upper limits. J.S.H. is supported by a NSERC discovery grant.

## REFERENCES

- Alpar, M. A. 2001, *ApJ*, 554, 1245
- Berestetskii, V. B., Lifshitz, E. M., & Pitaevskii, L. P. 1982, *Quantum Electrodynamics*, 2nd edn. (Oxford: Pergamon)
- Chatterjee, P., Hernquist, L., & Narayan, R. 2000, *ApJ*, 534, 373
- Corbet, R. H. D., Smale, A. P., Ozaki, M., Koyama, K., & Iwasawa, K. 1995, *ApJ*, 443, 786
- den Hartog, P. R., Kuiper, L., Hermsen, W., & Vink, J. 2004, *The Astronomer’s Telegram*, 293, 1
- Duncan, R. C. & Thompson, C. 1992, *ApJL*, 392, 9
- Ekşi, K. Y., Hernquist, L., & Narayan, R. 2005, *ArXiv Astrophysics e-prints*
- GLAST Facilities Science Team. 1999, *Announcement of Opportunity for GLAST*, Tech. rep., NASA, <http://glast.gsfc.nasa.gov/science/resources/aosrd/>
- Grenier, I. & Perrot, C. 2005, private comm. via Alice Harding
- Heisenberg, W. & Euler, H. 1936, *Z. Physik*, 98, 714
- Heyl, J. S. & Hernquist, L. 1997a, *Phys. Rev. D*, 55, 2449
- . 1997b, *Journ. Phys. A*, 30, 6485
- . 1997c, *ApJ*, 489, 67
- . 1997d, *ApJ*, 491, 95
- . 1998, *Phys. Rev. D*, 58, 043005
- . 1999, *Phys. Rev. D*, 59, 045005
- . 2005, *ApJ*, 618, 463 [Paper I]
- Heyl, J. S. & Kulkarni, S. R. 1998, *ApJ*, 506, 61
- Hulleman, F., van Kerkwijk, M. H., & Kulkarni, S. R. 2000, *Nature*, 408, 689
- Hurley, K. 2000, in *American Institute of Physics Conference Series*, 515
- Jung, G. V. 1989, *ApJ*, 338, 972
- Kuiper, L., Hermsen, W., & Mendez, M. 2004, *ApJ*, 613, 1173
- Menou, K., Perna, R. & Hernquist, L. 2001, *ApJ*, 559, 1032

- Mereghetti, S., Chiarlone, L., Israel, G. L., & Stella, L. 2002, in *Neutron Stars, Pulsars, and Supernova Remnants*, 29–+
- Mereghetti, S., Gotz, D., Mirabel, I. F., & Hurley, K. 2004a, *ArXiv Astrophysics e-prints*, astro-ph/0411695
- Mereghetti, S., Tiengo, A., Stella, L., Israel, G. L., Rea, N., Zane, S., & Oosterbroek, T. 2004b, *ApJ*, 608, 427
- Molkov, S., Hurley, K., Sunyaev, R., Shtykovsky, P., & Revnivtsev, M. 2004, *ArXiv Astrophysics e-prints*, astro-ph/0411696
- Özel, F. 2004, *ArXiv Astrophysics e-prints*, astro-ph/0404144
- Sanbonmatsu, K. Y. & Helfand, D. J. 1992, *AJ*, 104, 2189
- Thompson, C. & Duncan, R. C. 1995, *MNRAS*, 275, 255
- . 1996, *ApJ*, 473, 322
- Vasisht, G., Gotthelf, E. V., Torii, K., & Gaensler, B. M. 2000, *ApJ*, 542, L49